energies

MDPI

Influence of Hydrate-Forming Gas Pressure on Equilibrium Pore Water Content in Soils

Daria Sergeeva [1,*], Vladimir Istomin [1,2], Evgeny Chuvilin [1,*], Boris Bukhanov [1] and Natalia Sokolova [1]

[1] Center for Hydrocarbon Recovery, Skolkovo Innovation Center, Skolkovo Institute of Science and Technology (Skoltech), Bolshoi Boulevard 30b1, 121205 Moscow, Russia; V.Istomin@skoltech.ru (V.I.); B.Bukhanov@skoltech.ru (B.B.); N.Sokolova@skoltech.ru (N.S.)

[2] Scientific and Research Institute of Natural Gases and Gas Technologies (Gazprom VNIIGAZ), Building 1, Razvilka, Leninsky District, 142717 Moscow, Russia

[*] Correspondence: D.Sergeeva@skoltech.ru (D.S.); E.Chuvilin@skoltech.ru (E.C.)

Abstract: Natural gas hydrates (primarily methane hydrates) are considered to be an important and promising unconventional source of hydrocarbons. Most natural gas hydrate accumulations exist in pore space and are associated with reservoir rocks. Therefore, gas hydrate studies in porous media are of particular interest, as well as, the phase equilibria of pore hydrates, including the determination of equilibrium pore water content (nonclathrated water). Nonclathrated water is analogous to unfrozen water in permafrost soils and has a significant effect on the properties of hydrate-bearing reservoirs. Nonclathrated water content in hydrate-saturated porous media will depend on many factors: pressure, temperature, gas composition, the mineralization of pore water, etc. In this paper, the study is mostly focused on the effect of hydrate-forming gas pressure on nonclathrated water content in hydrate-bearing soils. To solve this problem, simple thermodynamic equations were proposed which require data on pore water activity (or unfrozen water content). Additionally, it is possible to recalculate the nonclathrated water content data from one hydrate-forming gas to another using the proposed thermodynamic equations. The comparison showed a sufficiently good agreement between the calculated nonclathrated water content and its direct measurements for investigated soils. The discrepancy was ~0.15 wt% and was comparable to the accuracy of direct measurements. It was established that the effect of gas pressure on nonclathrated water content is highly nonlinear. For example, the most pronounced effect of gas pressure on nonclathrated water content is observed in the range from equilibrium pressure to 6.0 MPa. The developed thermodynamic technique can be used for different hydrate-forming gases such as methane, ethane, propane, nitrogen, carbon dioxide, various gas mixtures, and natural gases.

Keywords: gas hydrates; porous media; pore water; nonclathrated water; ice; phase equilibria; thermodynamic calculations; kaolinite clay; methane

1. Introduction

The phase equilibrium problem of gas hydrates in porous media has a long history. Russian scientists first drew attention to this problem in the 1960s of the 20th century during the analysis of hydrate conditions in the oil and gas basins of the Siberian permafrost. The first experimental data concerning the existence of pore hydrate conditions were obtained by Makogon in the middle of the 60s of the last century to substantiate natural gas hydrate formations in reservoir rocks [1]. Those results showed that thermobaric conditions for pore hydrates can be different from bulk hydrates. Later, to understand the effect of porous media, a new parameter was added to the thermodynamic model of hydrate existence, which described as pore water in a single capillary of a given radius. In subsequent studies, a porous medium was also considered to be a system with an average capillary radius. As a rule, the value of $\cos(\theta)$ (θ is contact angle) for hydrophilic capillaries was taken to be unity. This model gives the value of the temperature shift of the hydrate formation curve

depending on capillary radius (the shift is increased while decreasing the capillary radius). This was followed by numerous attempts of experimental study on gas hydrate conditions in different porous media [2–14], as well as attempts to present theoretical estimations for the description of size distribution and its influence on phase equilibrium in a porous medium [14–27].

Nowadays, the theoretical approach for a real soil system of setting the pore space structure as a certain capillary size distribution and from this distribution calculating the thermodynamic properties of pore water has only methodological (or theoretical) significance [28]. This is since real porous media (sediments, soils, rocks) can be considered to be systems of capillaries or particle size distribution only on the qualitative level. Such a theoretical scheme has indeed had practical results for specially prepared model porous media with a narrow capillary size distribution, as considered in [15,28]. Therefore, for soil systems another approach is preferable in which the thermodynamic properties of pore water in a sample of porous media are measured depending on the water content of the sample. Such experimental data on pore water properties (measurements of pore water activity or unfrozen water content in the samples) make subsequent thermodynamic calculations of pore water content in equilibrium with gas, hydrate, and ice possible. Additional analysis showed that the effect of hydrate-forming gas pressure on nonclathrated water content was not previously covered. Below, our main task is to reveal the effect of pressure of a hydrate-forming gas on pore water content in the sample that is in equilibrium with gas hydrates at the temperature under consideration. Such pore water in soils/sediments is called nonclathrated water. Thus, nonclathrated water is liquid water in a sample of a porous medium (a soil or sediment system) at pressure P, which is in thermodynamic equilibrium with a hydrate-forming gas and a gas hydrate in a bulk phase. Pressure P must be greater than P_{eq}, the equilibrium pressure of hydrate formation (corresponding to equilibrium bulk water or ice–gas–gas hydrate). The term "nonclathrated water" was first introduced in our papers [29,30] by analogy with the concept of unfrozen water. Currently, this term is already used in the literature [31–33]. In contrast to unfrozen water, the concept of nonclathrated water is applicable to both negative and positive Celsius temperatures.

From general thermodynamic considerations, the amount of nonclathrated water in the soil sample decreases with an increase in the pressure of the hydrate-forming gas (part of the pore water transformed into a hydrate phase). As shown below, the effect of gas pressure on nonclathrated water content is highly nonlinear.

2. Analytical Dependences of Hydrate-Forming Gas Pressure Influence on Nonclathrated Water

For describing the thermodynamic properties of pore water, it is convenient to use water activity $a(T, W)$, which depends on the water content of the sample and temperature:

$$a = \frac{p_{wpor}}{p_w},\qquad(1)$$

where p_{wpor} is water vapor pressure over the soil sample with water content W (wt% water relative to the dry sample), and p_w is the pressure of saturated water vapor over the bulk water (in MPa or Pa).

The experimental determination of pore water activity $a = a(T, W)$, depending on water content W in the soil at or close to room temperature, can be carried out by various methods. The most efficient method is to measure the dew point of air brought into equilibrium with a wet soil sample with water content W, followed by a recalculation of the dew-point temperature to water vapor pressure over wet soil and, thereby, water activity. The method for measuring pore water activity is described in detail elsewhere [34].

The activity of pore water in a wet sample W depends on both the water content of the sample and on its temperature, i.e., $a = a(T, W)$. As a first approximation, the temperature dependence of pore water activity a (at a fixed W) can be neglected. However, this is not

the case for low water content in the soil, especially in the presence of a clay component with a sliding framework in the soil (for example, smectite).

Another task was to derive some thermodynamic dependencies connecting pore water activity in the soil (at atmospheric pressure) with the fugacity or pressure of the hydrate-forming gas at a given temperature. At the same time, it was necessary to separately describe positive and negative temperatures due to the existence of unfrozen water at negative Celsius temperatures. Unfrozen pore water in equilibrium with ice also exists at gas pressure, but gas pressure must be below pressure on the gas–ice–hydrate equilibrium line. At pressure P, higher pressure P_{eq} (pressure at the gas–ice–hydrate equilibrium line) exists instead of ice in the gas hydrate phase (the hydrate phase becomes stabler than the ice phase). Thus, pore water at pressure $P > P_{eq}$ should be nonclathrated water (according to the terminology considered in the introduction).

The consideration of a gas pressure effect on nonclathrated water content begins at positive Celsius temperatures. The soil sample is fixed at temperature $T > 273.15$ K (when deriving thermodynamic relations, it is more convenient to set the temperature in Kelvin, while in practical examples, it is more convenient to set the temperature in Celsius). Then, experimental data of pore water activity via the water content of sample W (i.e., dependence $a = a(W)$) were obtained. Then, the hydrate former was chosen (for example, gases such as methane, carbon dioxide, ethane, propane, nitrogen, their mixtures, and natural gas). The line of the three-phase gas–water (in bulk phase)–hydrate equilibrium was assumed either from experimental data or calculated using available software. For instance, in many books analytical approximations of three-phase equilibrium lines (gas and gas hydrates with water/ice) for pure gases were presented [35–37].

The pressure of hydrate formation P_{eq} at a given temperature T, gas fugacity f_{eq}, and gas compressibility factor z_{eq} were denoted assuming that the activity of pore water in sample $a = a(T, W) < 1$ was known from experimental measurements at atmospheric pressure. Water activity $a = 1$ corresponds to the bulk phase of water. At pressure $P < P_{eq}$, there was no gas hydrate in the system. At $P = P_{eq}$, the amount of nonclathrated water in sample W formally tended to infinity. We were interested in the thermodynamic relation between gas pressure P at the three phase equilibrium gas–pore water–hydrate ($P \geq P_{eq}$) and the activity of pore water $= a(T, W) < 1$, as well as the water content W of the soil sample.

A preliminary remark is that from the morphological studies of hydrates [38], the characteristic size of hydrate particles obtained in real soils, as a rule, exceeds 10 microns. It is easy to show that at a characteristic particle size of more than 1 micron, the thermodynamic properties of pore hydrate particles practically do not differ from their properties in the bulk phase. For further consideration, we excluded nanoporous media in which the thermodynamic properties of the pore hydrate could significantly differ from the properties of the bulk hydrate phase. The effect of a hydrate particle size of 0.1 microns or less on phase equilibrium requires special consideration.

According to the traditional thermodynamic model of clathrate hydrates by van der Waals–Platteeuw and Barrer–Stuart (see, for instance, [28]), the chemical potential of water $\mu_h(T, P)$ in the hydrate phase is written as follows:

$$\mu_h(T, P) = \mu_h^0(T, P_0) - \nu_1 RT \ln(1 + C_1 f) - \nu_2 RT \ln(1 + C_2 f) + V_h \cdot (P - P_0), \quad (2)$$

or, in an equivalent form:

$$\mu_h = \mu_h^0(T, P_0) + \nu_1 RT \ln(1 - \theta_1) + \nu_2 RT \ln(1 - \theta_2) + V_h \cdot (P - P_0),$$

where T—temperature, K; P—gas pressure, MPa; $P_0 = 0.101325$ MPa; V_h—molar volume of water in hydrate (22.61 cm^3/mol for cubic structure I and 23.06 cm^3/mol for cubic structure II); $\mu_h^0(T, P_0)$—chemical potential of water in an empty clathrate lattice at pressure P_0 and temperature T; $\mu_h(T, P)$—chemical potential of water in a clathrate lattice partially filled with guest molecules at pressure P and temperature T; R—universal gas constant,

$R = 8.3146$ J/(mol·K); $C_1 = C_1(T)$, $C_2 = C_2(T)$—Langmuir constants for large and small cavities (depending only on temperature), respectively; θ_1, θ_2—degrees of filling small and large cavities of the structure, respectively; ν_1 and ν_2—crystallochemical constants ($\nu_1 = \frac{1}{23}$ and $\nu_2 = \frac{3}{23}$ are for Structure I, and $\nu_1 = \frac{2}{17}$, $\nu_2 = \frac{1}{17}$ are for Structure II).

Quantities θ, C, and f are related by the Langmuir isotherm $\theta = C f / (1 + C f)$ (the traditional model assumes that gas molecules are sorbed by the clathrate lattice in accordance with the Langmuir isotherm). Hydrate numbers n in the chemical formulas of hydrates M·nH$_2$O, where M is a gas molecule (for example, CH$_4$), are also used below. Hydrate number n is expressed in terms of the degrees of filling cavities as follows: $n^I = \frac{23}{\theta_1^I + 3\theta_2^I}$, $n^{II} = \frac{17}{2\theta_1^{II} + \theta_2^{II}}$ for hydrate Structures I and II, respectively.

The chemical potential of water $\mu_w(T, P)$ in a pore solution in a good approximation can be written as follows:

$$\mu_w(T, P) = \mu_w^0(T, P_0) + RT \ln(1 - x) + RT \ln a + V_w \cdot (P - P_0), \tag{3}$$

where $\mu_w^0(T, P_0)$—chemical potential of pure bulk water at pressure P_0 and temperature T; $\mu_w(T, P)$—chemical potential of pore water in the soil sample at pressure P and temperature T; x—gas solubility in pore water; a—pore water activity in the soil sample measured at atmospheric pressure (pore water can also be saline); V_w—partial molar volume of water in pore solution, assuming that $V_w = 18.015$ cm^3/mol. Gas solubility in pore water can be approximately equal to solubility in the bulk water phase. In principle, the effect of a porous medium on gas solubility can be estimated by excluding that part of pore water volume in which the gas does not dissolve (for instance, water in the interlayer space of the sliding frame clays does not dissolve the gas).

Gas solubility in bulk water under gas pressure can be determined by the Krichevsky–Kazarnovsky equation [39] or calculated from the equations of state; experimental data can also be used. For calculations using equations of state, the cubic-plus-association (CPA) equation is recommended and is widely used in commercial software.

The Krichevsky–Kazarnovsky equation [39] for pure gas is

$$\ln \frac{f}{x} = \ln H + \frac{V_g(P - P_0)}{RT}, \tag{4}$$

where H, mol/(MPa·cm^3), Henry's coefficient of gas; V_g, partial molar volume of gas in water (cm^3/mol); f, gas fugacity, MPa (fugacity is determined by the equation of state and depends on temperature and pressure). Henry's coefficient H only depends on temperatures up to a pressure of 20–30 MPa. By knowing Henry's coefficient, gas fugacity f, and the partial molar volume V_g of gas in water, it is possible to determine molar fraction x of gas in water from Equation (4). Henry's coefficient is determined from experimental data on gas solubility in water, and the partial molar volume V_g may be determined from experimental data (V_g can also be measured in special direct volumetric experiments). Values of H and V_g for various gases are given in the literature [40].

For a gas mixture, the Krichevsky–Kazarnovsky equation is generalized as follows:

$$\ln \frac{f_j}{x_j} = \ln H_j + \frac{V_j(P - P_0)}{RT},$$

$$x = \sum_{j=1}^{N} x_j.$$

where N—amount of dissolved gases, x_j—mole fraction of j gas in water; H_j—Henry coefficient of j component of gas mixture; f_j—fugacity of j component of gas mixture, which is determined by the gas equation of state; V_j—partial molar volume of j gas in water.

Phase equilibrium gas–water bulk phase–hydrate at $P = P_{eq}$, $f = f_{eq}$ and a fixed temperature $T > 273.15$ corresponds to the equality of the chemical potential of water in

the hydrate phase according to Relation (2), and the chemical potential of water in the water bulk phase with dissolved gas according to Relation (3) at $a = 1$.

Equating the chemical potentials after some transformations, we obtain

$$\Delta\mu_{hw}^0(T, P_0) - v_1 RT \ln(1 + C_1 f_{eq}) - v_2 RT \ln(1 + C_2 f_{eq}) + V_h(P_{eq} - P_0) = V_w(P_{eq} - P_0) + RT \ln(1 - x_{eq})$$

or

$$\Delta\mu_{hw}^0(T, P_0) - v_1 RT \ln(1 + C_1 f_{eq}) - v_2 RT \ln(1 + C_2 f_{eq}) + \Delta V_{hw}(P_{eq} - P_0) - RT \ln(1 - x_{eq}) = 0, \tag{5}$$

where $\Delta\mu_{hw}^0(T, P_0) = \mu_h^0(T, P_0) - \mu_w^0(T, P_0)$—the difference between the chemical potentials of water in the hydrate phase, and liquid water at atmospheric pressure and considered temperature; $\Delta V_{hw} = V_h - V_w$, the difference between molar volumes of water in the hydrate lattice and in bulk water; $\Delta V_{hw} = 4.595$ and 5.045 cm^3/mol for cubic Structures I and II, respectively.

Let us consider phase equilibrium gas–pore water–hydrate at a given sample water content (moisture) W, i.e., at $P > P_{eq}$. In this case, the activity of pore water is equal to a ($a < 1$). Equating the chemical potentials of water in hydrate phase (2) and pore water solution (3), we obtain

$$\Delta\mu_{hw}^0(T, P_0) - v_1 RT \ln(1 + C_1 f) - v_2 RT \ln(1 + C_2 f) + V_h \cdot (P - P_0) = V_w \cdot (P - P_0) + RT \ln(1 - x) + RT \ln a$$

or

$$\Delta\mu_{hw}^0(T, P_0) - v_1 RT \ln(1 + C_1 f) - v_2 RT \ln(1 + C_2 f) + \Delta V_{hw} \cdot (P - P_0) - RT \ln(1 - x) - RT \ln a = 0 \tag{6}$$

Subtracting Relation (6) from (5) after some transformations,

$$v_1 RT \ln\left(\frac{1 + C_1 f}{1 + C_1 f_{eq}}\right) + v_2 RT \ln\left(\frac{1 + C_2 f}{1 + C_2 f_{eq}}\right) - \Delta V_{hw} \cdot (P - P_{eq}) + RT \ln\left(\frac{1 - x}{1 - x_{eq}}\right) + RT \ln a = 0 \tag{7}$$

Equation (7) relates pore water activity and consequently the water content W of the sample to gas fugacity f and gas pressure P at $P > P_{eq}$. In particular, from Equation (7) with $P = P_{eq}$, we obtain $RT \ln a = 0$ or $a = 1$ In Equation (7), quantity $\Delta\mu_{hw}^0(T, P_0)$ is excluded, but the value of equilibrium gas pressure P_{eq} is included (in comparison with (6)).

Equation (7) is easily generalized to the case of a gas mixture (natural or associated petroleum gas etc.); for this, in Equation (7) one should replace $C_1 f$ with $\sum_j C_{1j} f_j$ and $C_2 f$ with $\sum_j C_{2j} f_j$, where f_j, C_{1j}, C_{2j} are the fugacity and Langmuir constants of the j-th component of the gas mixture, respectively. For pure gases (propane, cyclopropane, and isobutane), small cavities of hydrate structure II are not filled, i.e., $\theta_1 = 0$ and $C_1 = 0$. In this case, the first term disappears from the left-hand side of Equation (7). The same is true for ethane hydrate, which forms Structure I (in ethane hydrate, the small cavities are also not filled).

At a gas pressure below 6–8 MPa, as an approximation its solubility in water (except for carbon dioxide) and the influence of the Poynting effect can be neglected (i.e., value $\Delta V_{hw}(P - P_{eq})$); then, we can obtain the following simplified relationship:

$$v_1 RT \ln\left(\frac{1 + C_1 f}{1 + C_1 f_{eq}}\right) + v_2 RT \ln\left(\frac{1 + C_2 f}{1 + C_2 f_{eq}}\right) + RT \ln a = 0 \tag{8}$$

or

$$\left(\frac{1 + C_1 f}{1 + C_1 f_{eq}}\right)^{v_1} \cdot \left(\frac{1 + C_2 f}{1 + C_2 f_{eq}}\right)^{v_2} = a^{-1} \tag{9}$$

Equations (8) and (9) can be used for methane, nitrogen, and inert gases at moderately high pressure levels (for CO_2, its water solubility should not be neglected).

Let us analyze the further possibilities of simplifying Relation (7) to reduce the necessary parameters for calculating nonclathrated water. For this, let us consider the nature

of cavities filling with gas molecules in hydrates of various structures. First, it should be considered that large cavities in clathrate structures are always almost completely occupied (i.e., the degree of the filling of large cavities is always close to unity, $\theta_2 \approx 1$). At temperatures close to 273 K for Structure I, $C_2 f > 10$ and for Structure II, $C_2 f > 50$. This yields the estimate of the large cavities' degree of filling at a temperature of $\sim$ 273 K: $\theta_2 > 0.9$ for Structure I and $\theta_2 > 0.97 - 0.98$ for Structure II. In addition, in many cases of practical interest (hydrates of methane, natural gases), the degree of the filling of small cavities of hydration structure θ_1 is also close to 1. With increasing temperature (and gas pressure), the degrees of filling approach unity.

Let us consider separately three practically important cases of the filling of clathrate cavities guest molecules: (i) $\theta_1 \approx 1$ and $\theta_2 \approx 1$; (ii) $\theta_1 = 0$, $\theta_2 \approx 1$; and (iii) $0 < \theta_1 < 1$, $\theta_2 \approx 1$.

Let the small and large cavities be almost filled, i.e., $\theta_1 \approx 1$, $C_1 f \gg 1$; $\theta_2 \approx 1$, $C_2 f \gg 1$. This situation is typical for methane and nitrogen gases and inert gases. Thus, we neglect the unit under the logarithm in expressions such as $\ln(1 + Cf)$, i.e., $\ln(1 + Cf) \approx \ln(Cf)$. Equation (7) is rewritten as follows:

$$\nu_1 RT \ln \frac{f}{f_{eq}} + \nu_2 RT \ln \frac{f}{f_{eq}} - \Delta V_{hw} \cdot (P - P_{eq}) + RT \ln \left(\frac{1-x}{1-x_{eq}} \right) + RT \ln a = 0$$

or

$$(\nu_1 + \nu_2) \ln \frac{f}{f_{eq}} = \frac{\Delta V_{hw} \cdot (P - P_{eq})}{RT} - \ln \left(\frac{1-x}{1-x_{eq}} \right) - \ln a \qquad (10)$$

For convenience, we introduce into consideration quantities

$$b = a(1-x) \exp \left(-\frac{\Delta V_{hw} \cdot (P - P_0)}{RT} \right), \quad b_{eq} = (1 - x_{eq}) \exp \left(-\frac{\Delta V_{hw} \cdot (P_{eq} - P_0)}{RT} \right) \qquad (11)$$

Let us rewrite (10), taking into account (11). After some transformations, we obtain

$$(\nu_1 + \nu_2) \ln \frac{f}{f_{eq}} = -\ln \frac{b}{b_{eq}} \text{ or } \ln \frac{f}{f_{eq}} = -\frac{1}{(\nu_1 + \nu_2)} \ln \frac{b}{b_{eq}},$$

and lastly,

$$\frac{f}{f_{eq}} = \left(\frac{b}{b_{eq}} \right)^{-\frac{1}{(\nu_1 + \nu_2)}} \qquad (12)$$

Relations (11) and (12) are the main result of the consideration of the thermodynamics when the filling of both types of cavities in gas hydrate structures is close to 1. Equation (12) allows for the given W and water activity a, and for the known values of P_{eq} and f_{eq}, to calculate the equilibrium gas fugacity f and gas pressure P. At a given gas pressure P, we may determine fugacity f and then the activity of pore water a and W. When calculating nonclathrated water content using Relation (12), no information is required on the thermodynamics of an empty clathrate lattice and the Langmuir constants of guest molecules (in contrast to Relation (10)).

If the gas is considered to be in the ideal gaseous state, then $f = P$, and Equation (12) can be rewritten as

$$\frac{P}{P_{eq}} = \left(\frac{b}{b_{eq}} \right)^{-\frac{1}{(\nu_1 + \nu_2)}} \qquad (13)$$

Since, as a first approximation, $\frac{b}{b_{eq}} \approx a$, then from Equation (13), a strong nonlinear relationship between a and $\frac{P}{P_{eq}}$ becomes obvious. Thus, it seems from the obtained relations that, with increasing pressure, the content of nonclathrated water in a porous medium sharply decreases and is in accordance with a power law.

If the gas under consideration is weakly nonideal (for example, for methane up to pressures of about 7–8 MPa), then the approximate thermodynamic formula $f \approx z(P){\cdot}P$ should be used, where z is the gas compressibility factor. By using it, Relation (12) is rewritten as

$$\frac{P}{P_{eq}} \approx \frac{z_{eq}}{z}{\cdot}\left(\frac{b}{b_{eq}}\right)^{-\frac{1}{(v_1+v_2)}},\qquad(14)$$

where $z = z(P)$, $z_{eq} = z(P_{eq})$ are factors of gas compressibility at pressure P and P_{eq}, respectively.

Let the large cavities be almost filled, $\theta_2 \approx 1$ $(C_2 f \gg 1)$ with empty small cavities, $\theta_1 = 0$. This case is realized for hydrates of propane, isobutane, cyclopropane, ethane, and their mixtures. Taking $v_1 = 0$, from Relation (12) we obtain

$$\frac{f}{f_{eq}} = \left(\frac{b}{b_{eq}}\right)^{-\frac{1}{v_2}}\qquad(15)$$

For the hydrate of Structure I (for instance, ethane): $v_2 = 3/23$, and for hydrates of Structure II (for propane and isobutane): $v_2 = 1/17$.

More approximate relationships occur:

$$\frac{P}{P_{eq}} \approx \frac{z_{eq}}{z}{\cdot}\left(\frac{b}{b_{eq}}\right)^{-\frac{1}{v_2}} \text{ and } \frac{P}{P_{eq}} = \left(\frac{b}{b_{eq}}\right)^{-\frac{1}{v_2}}.\qquad(16)$$

Let both cavities be filled, and the degree of the filling of large cavities is close to unity, $\theta_2 \approx 1$ $(C_2 f \gg 1)$, but the degree of the filling of small cavities θ_1 can vary over a wide range (from 0 to 1). A typical example is carbon dioxide hydrate (and in its mixtures with propane, isobutane, and ethane). In such cases, Expression (7) is transformed into the following form:

$$v_1 RT \ln\left(\frac{1+C_1 f}{1+C_1 f_{eq}}\right) + v_2 RT \ln \frac{f}{f_{eq}} - \Delta V_{hw}{\cdot}\left(P - P_{eq}\right) + RT \ln\left(\frac{1-x}{1-x_{eq}}\right) + RT \ln a = 0\qquad(17)$$

Considering that $\theta = \frac{Cf}{1+Cf}$ and $C = \frac{\theta}{f(1-\theta)}$, after some transformations, we lastly obtain

$$(1+C_1 f)^{v_1}{\cdot}f^{v_2} = (1+C_1 f_{eq})^{v_1}{\cdot}f_{eq}{}^{v_2}{\cdot}exp\left(\frac{\Delta V_{hw}{\cdot}\left(P - P_{eq}\right)}{RT}\right){\cdot}\left(\frac{1-x_{eq}}{a{\cdot}(1-x)}\right)\qquad(18)$$

Expression (18) is less convenient for practical use, since the Langmuir constant C_1 of a small cavity remains. Therefore, the question arises whether it is possible to also use Equations (12)–(14) for the hydrate of carbon dioxide, substituting stoichiometric value $1/(v_1 + v_2)$ for the actual (or effective) hydrate numbers n. In this version, Equations (12)–(14) are rewritten as follows:

$$\frac{f}{f_{eq}} = \left(\frac{b}{b_{eq}}\right)^{-n}\qquad(19)$$

More approximately,

$$\frac{P}{P_{eq}} \approx \frac{z_{eq}}{z}{\cdot}\left(\frac{b}{b_{eq}}\right)^{-n}, \frac{P}{P_{eq}} \approx \left(\frac{b}{b_{eq}}\right)^{-n} \approx \left(\frac{a}{a_{eq}}\right)^{-n},\qquad(20)$$

where n is the actual or effective hydrate number on the three-phase gas–bulk phase of water–hydrate equilibrium line.

The simplest Approximation (20) may only be used for low pressure levels and low gas solubility in water.

A numerical comparison of approximate Relations (18) and (19) with general thermodynamic Relation (7) showed that it is practically acceptable to use the actual hydrate number n (see below). Moreover, the numerical comparison of (7), (12), and (19) for methane and nitrogen hydrates (the case when both cavities are strongly filled) also showed the benefit of using Equation (20). At the same time, for hydrates in which only large cavities are strongly filled (ethane, propane, isobutane), stoichiometric hydrate numbers ($n = 23/3 = 7.67$ for ethane and $n = 17$ for propane and isobutane) should be used. Thus, the above-obtained approximate Relations (12–14) can be empirically improved by using Equations (19) and (20) with an effective hydrate number n (see below for the practical recommendations for choosing the values of n).

As a result, for the equilibrium of gas–pore water–gas hydrate, we obtained approximate Relations (12)–(20), which are convenient for practical applications. These relations were considered for positive temperatures in Celsius, but with some modifications they are applicable for temperatures below zero Celsius.

Let us discuss the thermodynamic correlations for calculating nonclathrated water content at temperatures below freezing Celsius. First, if at negative temperatures, the three-phase equilibrium of gas–bulk supercooled water–hydrate is used as a reference line (a continuous continuation of the line of gas–bulk water–hydrate to negative temperatures), then Relations (12)–(20) can also be applied for negative temperatures. However, the lines of the metastable three-phase equilibrium of gas–supercooled water–hydrate can be experimentally obtained only for small water droplets in especially organized experiments. Such unique data were obtained in the papers of Melnikov et al. [41,42] for methane, propane, and carbon dioxide gases. For other gases, up-to-date experimental information is not yet available. However, these lines (including those for ethane, isobutane, and gas mixtures) can be calculated with acceptable accuracy at least up to $-15\ °C$ using software by Istomin et al. [43]. In other software, calculations of metastable phase equilibria of gas hydrates as a rule are not provided. Second, the pressure range from P_{eq} to pressure, corresponding to the equilibrium of the gas hydrate with ice (this pressure note by P_{eq}^{ice}), calculated using relations of type (12), refers to the zone of nonclathrated water metastability (i.e., to a hypothetical situation, as if ice in a given system did not exist). Strictly speaking, calculations of the content of nonclathrated water at temperatures below $0\ °C$ should be carried out only for pressures $P > P_{eq}^{ice}$ (when there is no ice in the system because the ice is already transformed to hydrate phase).

Therefore, for thermodynamic calculations of nonclathrated water content at negative temperatures, it is preferable to use the gas–ice–hydrate line as reference. The advantage of this reference line is because cages' filling and the hydrate number n along this line vary very slightly, with temperatures ranging from -15 to $0\ °C$. In a soil system, pore water as a fourth phase also exists in the equilibrium with ice, hydrate, and gas (the locus of quadrupole points). At the quadrupole point, according to the above accepted terminology, pore water may simultaneously be considered as unfrozen and nonclathrated water. At this line, the value of pore water activity $a_{eq} = a_{eq}\ (t)$ describes the equilibrium between ice and pore water at atmospheric pressure. Thus, a_{eq} decreases with a decreasing negative temperature ($a_{eq}\ (t) < 1$).

This situation is illustrated in Figure 1. Bold lines are the lines of the three-phase equilibrium of gas–water or ice bulk phase–hydrate. Above these lines, there is a zone of nonclathrated pore water. Dotted lines are the equilibrium of gas–hydrate–nonclathrated water with given activity a of pore water (activity measured at atmospheric pressure). For positive Celsius temperatures at $P = P_{eq}$, value $a = 1$ and the amount of nonclathrated water formally become infinite. At $P > P_{eq}$, value $a < 1$, and when gas pressure P increases, pore water activity a and equilibrium water content W in the sample decrease.
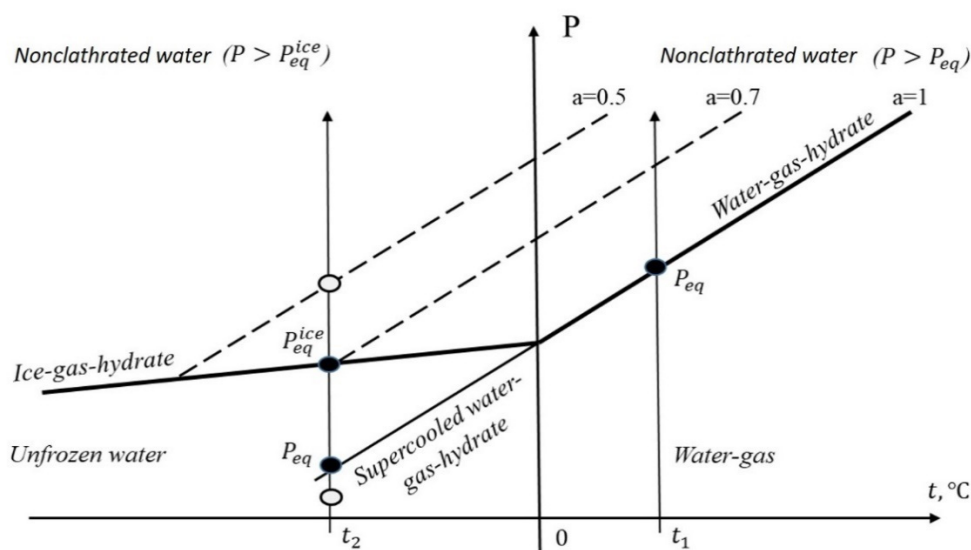
Figure 1. Unfrozen and nonclathrated water P-T conditions in porous media. Bold lines: three-phase gas–ice or supercooled water–hydrate equilibrium line; dotted lines: three-phase gas–water–hydrate equilibrium line at given pore-water activity.

At a given negative Celsius temperature with gas pressure increasing, the amount of unfrozen pore water (gas–pore water–ice equilibrium) increases up to the quadrupole point (at $P = P_{eq}^{ice}$), but very slowly. During a further increase in pressure ($P > P_{eq}^{ice}$), the content of nonclathrated pore water begins to sharply decrease (according to a power law as established above).

Thus, at temperatures below 0 °C, it is preferable to use the gas–ice–hydrate line as a reference line. Repeating the derivation of Relations (7)–(12), instead of Relation (12), the modified equation may be obtained. In Relation (12), P_{eq} should be replaced by P_{eq}^{ice} and f_{eq} by f_{eq}^{ice}; in Relation (11), value b should be replaced by b^{ice}, b_{eq} should be replaced by b_{eq}^{ice}, and ΔV_{hw} by $\Delta V_{hi} = V_h - V_i$, where V_i is the molar volume of ice ($19.65 \text{cm}^3/\text{mol}$).

As a result, using the curve gas–ice–hydrate equilibrium as a reference line, we obtain the following final equation:

$$\frac{f}{f_{eq}^{ice}} = \left(\frac{b^{ice}}{b_{eq}^{ice}}\right)^{-n},$$

(21)

where

$$b^{ice} = a(1-x)\exp\left(-\frac{\Delta V_{hi}\cdot(P-P_0)}{RT}\right), \; a < a_{eq};$$

$$b_{eq}^{ice} = a_{eq}\,(1-x_{eq})\exp\left(-\frac{\Delta V_{hi}\cdot(P_{eq}-P_0)}{RT}\right),$$

and $\Delta V_{hi} = V_h - V_i = 2.96$ and $3.41 \text{ cm}^3/\text{mol}$ for hydrate cubic structures I and II, respectively.

At low pressure, instead of Equation (21), the approximation may also be used

$$\frac{P}{P_{eq}^{ice}} \approx \frac{z_{eq}}{z}\cdot\left(\frac{b^{ice}}{b_{eq}^{ice}}\right)^{-n}, \; \frac{P}{P_{eq}^{ice}} \approx \left(\frac{b^{ice}}{b_{eq}}\right)^{-n} \approx \left(\frac{a^{ice}}{a_{eq}}\right)^{-n}$$

(22)

A new value a_{eq} appears in the definition of b_{eq}^{ice}, and it is essential that a_{eq} be a function of temperature, i.e., a_{eq} corresponding to the equilibrium of ice–unfrozen water in the soil under consideration (at atmospheric pressure). This means that for the practical application of Equation (21), it is necessary to determine the value of a_{eq}, depending on the temperature (negative in Celsius). Such dependence was obtained [44] for unfrozen water calculations (equilibrium of pore water and ice):

$$-RT \ln a_{eq} = 6008 \cdot (1 - T/T_o) - 38.2 \cdot \left[T \ln \frac{T}{T_o} + (T_o - T) \right]; \ T_o = 273.15 \text{ K}; \ (T < T_o) \tag{23}$$

Then Equation (23) was transformed into relationship between temperature t (in degrees Celsius) and pore water activity a_{eq} on the pore water–ice equilibrium line [34]:

$$t = 103.25 \ln a_{eq} + 5.57 (1 - a_{eq})^2 \tag{24}$$

Equation (24) is used to calculate unfrozen water content from measured water activity when the temperature is set to Celsius. However, for our purposes, a_{eq} needs to be expressed as a function of temperature t (in degrees Celsius). By the approximation of Equation (23), we may obtain

$$a_{eq} = 1 + 9.6768 \cdot 10^{-3} \cdot t_{eq} + 4.1769 \cdot 10^{-5} \cdot t_{eq}^2. \tag{25}$$

Dependencies (23) and (25) can both be used in calculating nonclathrated water content at negative temperatures from Relation (21). Thus, the final Equation (21) is supplemented by Relation (23) or (25).

3. Nonclathrated Water Content Calculation

In the above, some thermodynamic relations were obtained (Equations (6), (7), (13) and (19)–(25)) that make it possible to calculate nonclathrated water content in a soil sample at a given temperature, depending on the pressure of hydrate-forming gas.

First, the main Equation (6) allows for the performance of thermodynamic calculations of equilibrium gas fugacity f and then pressure P at a given temperature, depending on pore water activity a, and thereby pore water content W. However, for the application of Equation (6) in practice, we need to know (i) the structure of the hydrate, (ii) the thermodynamic properties of the empty clathrate lattice $\Delta \mu_{hw}^0(T, P_0) = \mu_h^0(T, P_0) - \mu_w^0(T, P_0)$, and (iii) the Langmuir constants of the hydrate-forming gas under consideration. These values can be obtained if the hydrate-phase thermodynamic model's parameterization is published and/or described in the software documentation. For example, such data were presented in Istomin et al. (1996), but for other software they are not documented as a rule.

Equation (7) also allows, at a given temperature T, known Langmuir constants C_1, C_2, and the value of P_{eq}, for calculating water activity a depending on gas pressure P under consideration, and thereby determining the content of nonclathrated water W in the sample. Equation (7) excludes information about the thermodynamics of the empty hydrate lattice $\Delta \mu_{hw}^0(T, P_0)$ but contains additional information on equilibrium gas pressure P_{eq}. However, from a practical point of view Equations (6)–(8) are not fully convenient, since the temperature dependences of the Langmuir constants for small and large cavities need to be specified for the considered hydrate-forming gas (these constants must also be consistent with the three-phase equilibrium lines). Thus, relations such as Equation (13) look more attractive from a practical point of view, but they are only a good approximation of the main thermodynamic Relations (6) and (7). Numerical analysis showed that a small additional correction of equations such as (13) can be made with the replacement of the limiting hydrate number $\frac{1}{(\nu_1 + \nu_2)}$ by its effective value n.

As a result, for the practical calculations of the nonclathrated water content, Relations (19) and (20) are recommended at temperatures above 0 °C, and Relations (21) and (23) (or (25)) at temperatures below 0 °C. For rough estimations, the replacement of gas fugacity f by $z \cdot P$ in the equation is possible. This approximation may be used for methane up to a pressure of 7–8 MPa.

Hydrate numbers n for different gases are shown in Tables 1 and 2 (for positive and negative Celsius temperatures, respectively) that were calculated by using software [43]. For C_3H_8 and i-C_4H_{10}, a limited hydrate number may be used.

Table 1. Hydrate numbers n for some gases at T > 273 K on three-phase gas–water–hydrate equilibrium line.

Hydrate-Forming Gas	Hydrate Numbers n in Equations (19) and (20) at Temperatures T (K)		
	273.15	278.15	283.15
CH_4	6.05	5.98	5.93
C_2H_6	7.77	7.74	7.72
C_3H_8	17	17	17
i-C_4H_{10}	17	17	17
N_2	6.18	6.00	5.90

Table 2. Hydrate numbers for some gases at T < 273 K on three-phase gas–ice–hydrate equilibrium line of.

Hydrate-Forming Gas	Hydrate Numbers n in Equations (21) at Temperatures T (K)		
	258.15	263.15	268.15
CH_4	6.01	6.03	6.04
C_2H_6	7.75	7.76	7.76
C_3H_8	17	17	17
i-C_4H_{10}	17	17	17
N_2	6.19	6.21	6.23

A variant of the calculation is also possible if the unfrozen water content in frozen soils for different temperature levels ($W_{unf}(t)$) is known from the experiment. Using Equation (25), we immediately establish the dependence of pore water activity a on the water content W of the sample. Then, we may calculate the nonclathrated water content as a function of W for any hydrate-forming gas and any temperature (at a negative Celsius temperature according to Relations (21), (23), and (25) and at a positive Celsius temperature according to Relations (19) and (20)).

Using the proposed technique, the pressure dependence of the nonclathrated water content was calculated at a temperature of 265.65 K in a kaolinite clay and sand–clay mixture samples (sand plus 14% kaolinite clay and sand plus 25% kaolinite clay). This kaolinite clay was used previously to determine the effect of temperature on nonclathrated water content in porous media [28]. Soil characteristics are presented in Table 3.

Table 3. Soil characteristics.

Soil Type	Particle Size Distribution (%)							Mineralogy (%)		Salinity (%)
	1–0.5 (mm)	0.5–0.25 (mm)	0.25–0.1 (mm)	0.1–0.05 (mm)	0.05–0.01 (mm)	0.01–0.002 (mm)	<0.002 (mm)			
Sand	0.2	35.7	62.9	0.8	0.3	0.1		Quartz	>90	<0.01
Kaolinite clay	0.7	0.5	0.4	2.9	19.5	34.0	42.0	Kaolinite Quartz Muscovite	92 62	0.04

Sand consists of quartz (more than 90%) the prevailing fraction of sand particles 0.1–0.25 mm is reach 62.9%. Kaolinite clay consists mainly of kaolinite (92%), with 95.5% silt-clay size particles, while the percentage of clay particles (<0.002 mm) reaches 42%. Kaolinite clay contains minor amounts of dissolved salts (0.04%). The specific active surface areas of sand and kaolinite clay defined by nitrogen adsorption are 0.2 and 12 m^2/g, respectively.

First, experimental data of pore water activity a at atmospheric pressure via water content W were obtained (Table 4).

Table 4. Experimental data on the water activity *a* of kaolinite clay via different water content (W) levels at 298.15 K and atmospheric pressure.

W (wt%)	a	W (wt%)	a	W (wt%)	a
28.86	0.995	6.41	0.972	2.20	0.897
21.80	0.993	5.42	0.967	1.81	0.866
17.70	0.990	5.12	0.963	1.53	0.830
16.72	0.990	4.07	0.953	1.45	0.813
12.47	0.986	3.55	0.943	1.25	0.753
8.15	0.978	2.79	0.924	1.18	0.720

Pore water activity *a* was determined with a WP4-T device by a method previously described in detail [28,34].

Thermodynamic calculations of nonclathrated water were carried out using four methods (Figure 2 and Table 5):

- Equation (7), the most precise method, where the Langmuir constants were obtained from ratio $C = \theta/(1 - \theta)/f$, and the degree of cavity filling was calculated using our software [43].
- Equations (11) and (19), where the three-phase methane–supercooled water–hydrate equilibrium line was used as a reference line, $P_{eq} = 1.26$ MPa and *n*=5.75.
- Equation (21) and $n = 5.75$, where the three-phase gas–ice–hydrate equilibrium line was used as a reference line, $P_{eq}^{ice} = 2.00$ MPa and $n = 5.75$.
- Equations (21) and (25), where the three-phase gas–ice–hydrate equilibrium line was used as a reference line, $P_{eq}^{ice} = 2.00$ MPa, $n = 6.03$.

In Figure 2, equilibrium pressure $P_{eq}^{ice} = 2.00$ MPa on the ice–methane–hydrate equilibrium line at a temperature of 265.65 K.

The Equation (21) approximation with $n = 6.03$ gave a very similar result to that of fully correct Equation (7). This means that at negative temperatures, it is preferable to use ice–gas–hydrate as a reference line and actual hydrate numbers from Table 2. For positive temperatures, Equation (19) and actual hydrate numbers from Table 1 are recommended.

The data (Table 4) were calculated using measured water activities for kaolinite clay (Table 3). Three methods were used: squares—general (most accurate) Equation (7); crosses—approximate Equation (19), considering (11); triangles according to approximate Equation (21) using three-phase equilibrium gas–ice–hydrate as a reference line; circles—also according to Equation (21) with a hydrate number $n = 6.03$.

A comparison of calculated data with direct experimental data obtained by the contact method (Table 6) is shown in Figure 2.

The contact method is a direct technique for nonclathrated water content determination in soil samples. It was proposed earlier in our papers [45,46]. Nonclathrated water content data has a good agreement between that calculated by thermodynamic equations and experimental data obtained by the contact method, the accuracy of which is about 0.1 wt% [28]. The largest discrepancy of ~0.15 wt% in the data was observed in the range of 1.4–1.5 wt%.

Additional experimental data and calculations of nonclathrated water content were obtained for sand–clay mixtures, which consist of quartz sand and 14 wt% and 25 wt% of kaolinite clay, respectively (Figure 3). These results also demonstrate a good agreement between the calculation and the experimental data. There is a regular increase in the amount of nonclathrated water in model soils with the increase in the content of clay particles. For example, the content of nonclathrated water at 4 MPa gas pressure in sand with 14 wt% kaolinite clay is 0.25%, which is two times lower than that in the sand with 25 wt% clay. The effect of gas pressure on the nonclathrated water content is weak at pressures above 6–8 MPa. However, the difference depending on the content of clay particles is also preserved under these conditions.
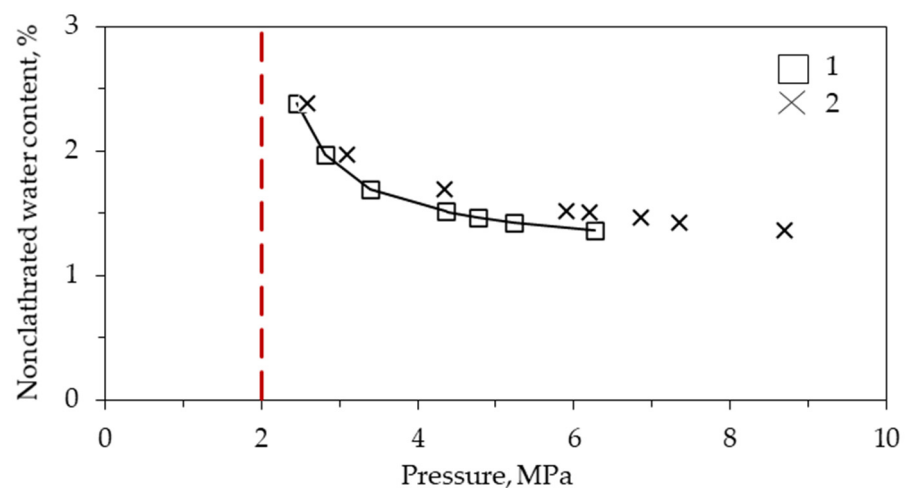
Thus, the proposed thermodynamic technique for nonclathrated water content calculation allows one to estimate the effect of hydrate-forming gas pressure on the equilibrium water content in hydrate-bearing soil samples. The comparison showed a sufficiently good agreement between the calculated results by the proposed technique with the direct measurements of nonclathrated water for all investigated soils.

Table 5. Dependence of nonclathrated water content in kaolinite clay on methane pressure at a temperature of 265.65 K by different calculations.

W (%)	P, MPa by Equation (7)	P, MPa (Equilibrium Gas-Supercooled Water-Hydrate by Equation (19) at $n = 5.75$)	P, MPa (Equilibrium Gas-Ice-Hydrate by Equation (21) at $n = 5.75$)	P, MPa (Equilibrium Gas-Ice-Hydrate by Equation (21) at $n = 6.03$)
2.79	2.10	2.06	2.07	2.08
2.20	2.56	2.49	2.49	2.52
1.81	3.24	3.13	3.11	3.18
1.53	4.33	4.15	4.10	4.26
1.45	5.01	4.80	4.71	4.93
1.25	9.03	8.60	8.18	8.91

Table 6. Experimental data for determination of nonclathrated water at $P > P_{eq}^{ice} = 2.00$ MPa, obtained by contact method for kaolinite clay and its calculations by using Equation (21) and $n = 6.033$ at 265.65 K temperature.

Nonclathrated Water Content (%)	P, MPa (Experimental Data)	P, MPa (Thermodynamic Calculations)
1.36	8.69	6.27
1.43	7.35	5.23
1.47	6.85	4.77
1.51	6.2	4.40
1.52	5.9	4.36
1.69	4.34	3.39
1.97	3.10	2.82
2.38	2.59	2.46

Figure 2. Change in nonclathrated water content depending on methane pressure in kaolinite clay at a temperature of 265.65 K. Calculated data represented by squares—1. Crosses, experimental data—2. Solid line—approximation of calculated data; red line—equilibrium "ice–methane–hydrate" at a temperature of 265.65 K.
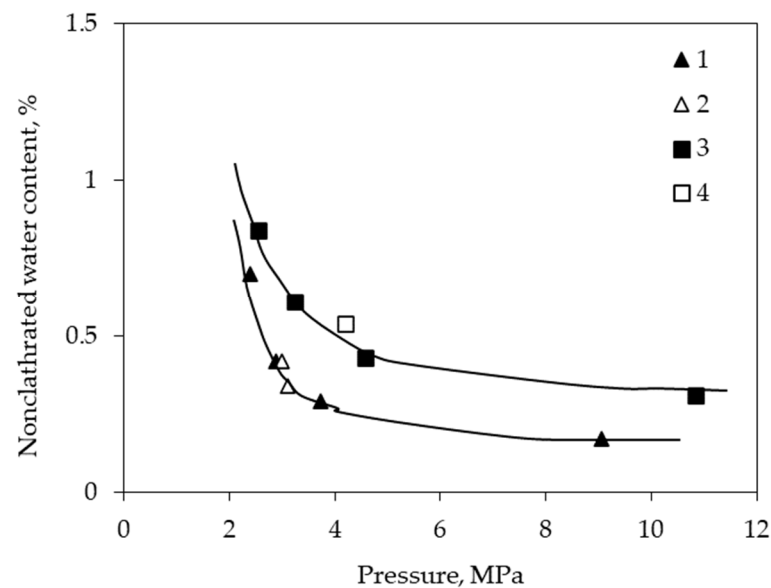
Figure 3. Change of nonclathrated water content depending on methane pressure in artificial sediment mixtures: sand with 14% (1, 2) and 25% (3, 4) kaolinite particles at 268.15 K. 1,3—Calculated data and 2,4—experimental data. P_{eq} = 2.36 MPa (CH$_4$).

The obtained methodological results make it possible to use the proposed technique during the efficiency estimation of methane hydrate recovery by various production methods. In contrast to the conventional approach, which takes into account only the temperature shift for the assessment of hydrate conditions in porous media, the investigated method takes into account the increase in equilibrium pore water content (non-clathrated water) due to reservoir pressure rise. The information about residual water (nonclathrated water) in hydrate-saturated reservoirs is very important for predicting the efficiency of CO$_2$ sequestration in a hydrate form under definite temperature and pressure conditions.

4. Conclusions

Currently, studies of the phase composition of hydrate-containing rocks are very important for stability conditions of natural hydrate reservoirs and hydrate production technologies. One of the main aspects is associated with the equilibrium liquid phase of water in hydrate-bearing rocks (nonclathrated water), the content of which affects their reservoir properties and behavior. This study is focused on a simplified isothermal thermodynamic model for the calculation of nonclathrated water content in hydrate-bearing porous media at various hydrate-forming gas pressures. Some analytical equations for the influence of gas pressure on nonclathrated water content both for negative and positive temperatures were obtained. Qualitative regularities were considered. When the pressure of hydrate-forming gas increased, the content of nonclathrated water significantly decreased by power law. That is why the pressure dependence of nonclathrated water content is strongly nonlinear.

The final analytical equations are very simple and include only two parameters for low gas pressure: gas pressure in gas hydrate with bulk water (or ice) equilibrium and hydrate number. For higher gas pressure, values of fugacity may be used instead of pressure, and the Poynting correction and gas solubility in water may be included. The proposed equations gave a very similar result in comparison to that of the strong approach and may be used in practice for rapid calculations. To apply the proposed equations for the determination of the content of nonclathrated water, it is necessary to input experimental data on the pore water activity in a sample as a function of the water content at atmospheric pressure. Water activity data may also be recovered from unfrozen water contents for the soil at different negative temperatures. The known nonclathrated water content for

one hydrate-forming gas is possible to be recalculated into nonclathrated water content for another hydrate forming gas. For such calculations, we need only gas fugacity and solubility in pore water.

The calculations of the nonclathrated water content for methane-saturated kaolinite clay and sandy clay mixtures showed sufficiently good agreement between the results obtained by the proposed method and the contact method for the direct experimental determination of nonclathrated water content. The largest discrepancy was observed in the water content range of 1.4–1.7 wt%, and it was ~0.15 wt%. This value of variance is comparable to the accuracy of the contact method. Additionally, the most pronounced effect of a gas pressure on nonclathrated water content is observed in the range from equilibrium pressure to 6 MPa, and with further pressure increases this effect is insignificant. As a result, the proposed thermodynamic technique is convenient for practical calculations and could potentially be used for different hydrate-forming gases (methane, ethane, propane, nitrogen, carbon dioxide, gas mixtures, and natural gases) and soils.

Conflicts of Interest: The authors declare no conflict of interest.

References

1. Makogon, Y.F. *Hydrates of Natural Gases*; Nedra: Moscow, Russia, 1974; 208p. (In Russian)
2. Handa, Y.P.; Stupin, D.Y. Thermodynamic properties and dissociation characteristics of methane and propane hydrates in 70-.ANG.-radius silica gel pores. *J. Phys. Chem.* **1992**, *96*, 8599–8603. [CrossRef]
3. Uchida, T.; Ebinuma, T.; Ishizaki, T. Dissociation condition measurements of methane hydrate in confined small pores of porous glass. *J. Phys. Chem. B* **1999**, *103*, 3659–3662. [CrossRef]
4. Seo, Y.; Lee, H.; Uchida, T. Methane and carbon dioxide hydrate phase behavior in small porous silica gels: Three-phase equilibrium determination and thermodynamic modeling. *Langmuir* **2002**, *18*, 9164–9170. [CrossRef]
5. Anderson, R.; Llamedo, M.; Tohidi, B.; Burgass, R.W. Experimental measurement of methane and carbon dioxide clathrate hydrate equilibria in mesoporous silica. *J. Phys. Chem. B* **2003**, *107*, 3507–3514. [CrossRef]
6. Uchida, T.; Ebinuma, T.; Takeya, S.; Nagao, J.; Narita, H. Effects of pore sizes on dissociation temperatures and pressures of methane, carbon dioxide and propane hydrate in porous media. *J. Phys. Chem. B* **2002**, *106*, 820–826. [CrossRef]
7. Uchida, T.; Takeya, S.; Chuvilin, E.M.; Ohmura, R.; Nagao, J.; Yakushev, V.S.; Istomin, V.A.; Minagawa, H.; Ebinuma, T.; Narita, H. Decomposition of methane hydrates in sand, sandstone, clays and glass beads. *J. Geophys. Res.* **2004**, *109*, B05206. [CrossRef]
8. Kang, S.P.; Lee, J.W.; Ryu, H.J. Phase behavior of methane and carbon dioxide hydrates in meso- and macro-sized porous media. *Fluid Phase Equilibria* **2008**, *274*, 68–72. [CrossRef]
9. Smith, D.H.; Seshadri, K.; Uchida, T.; Wilder, J.W. Thermodynamics of methane, propane, and carbon dioxide hydrates in porous glass. *AICHE J.* **2004**, *7*, 1589–1598. [CrossRef]
10. Chong, Z.R.; Yang, M.; Khoo, B.C.; Linga, P. Size effect of porous media on methane hydrate formation and dissociation in an excess gas environment. *Ind. Eng. Chem. Res.* **2016**, *55*, 7981–7991. [CrossRef]
11. Zarifi, M.; Javanmardi, J.; Hashemi, H.; Eslamimanesh, A.; Mohammadi, A.H. Experimental study and thermodynamic modelling of methane and mixed $C_1 + C_2 + C_3$ clathrate hydrates in the presence of mesoporous silica gel. *Fluid Phase Equilibria* **2016**, *423*, 17–24. [CrossRef]
12. Park, T.; Lee, J.Y.; Kwon, T.H. Effect of pore size distribution on dissociation temperature depression and phase boundary shift of gas hydrate in various fine-grained sediments. *Energy Fuels* **2018**, *32*, 5321–5330. [CrossRef]
13. Em, Y.; Stoporev, A.; Semenov, A.; Glotov, A.; Smirnova, E.; Villevald, G.; Lvov, Y. Methane hydrate formation in halloysite clay nanotubes. *ACS Sustain. Chem. Eng.* **2020**, *8*, 7860–7868. [CrossRef]

14. Zaripova, Y.; Yarkovoi, V.; Varfolomeev, M.; Kadyrov, R.; Stoporev, A. Influence of water saturation, grain size of quartz sand and hydrate-former on the gas hydrate formation. *Energies* **2021**, *14*, 1272. [CrossRef]

15. Clarke, M.A.; Pooladi-Darvish, M.; Bishnoi, P.R. A method to predict equilibrium conditions of gas hydrate formation in porous media. *Ind. Eng. Chem. Res.* **1999**, *38*, 2485–2490. [CrossRef]

16. Klauda, J.B.; Sandler, S.I. Modeling gas hydrate phase equilibria in laboratory and natural porous media. *Ind. Eng. Chem. Res.* **2001**, *40*, 4197–4208. [CrossRef]

17. Wilder, J.W.; Seshadri, K.; Smith, D.H. Modeling hydrate formation in media with broad pore size distributions. *Langmuir* **2001**, *17*, 6729–6735. [CrossRef]

18. Mel'nikov, V.P.; Nesterov, A.N. Gas hydrate formation from porous mineralized water. *Earth's Cryosphere* **2001**, *1*, 61–67. (In Russian)

19. Smith, D.H.; Wilder, J.W.; Seshadri, K. Methane hydrate equilibria in silica gels with broad pore-size distributions. *AICHE J.* **2002**, *2*, 393–400. [CrossRef]

20. Li, X.S.; Zhang, Y.; Li, G.; Chen, Z.Y.; Yan, K.F.; Li, Q.P. Gas hydrate equilibrium dissociation conditions in porous media using two thermodynamic approaches. *J. Chem. Thermodyn.* **2008**, *40*, 1464–1474. [CrossRef]

21. Chen, L.T.; Sun, C.Y.; Chen, G.J.; Nie, Y.Q. Thermodynamics model of predicting gas hydrate in porous media based on reaction-adsorption two-step formation mechanism. *Ind. Eng. Chem. Res.* **2010**, *49*, 3936–3943. [CrossRef]

22. Lee, S.; Seo, Y. Experimental measurement and thermodynamic modeling of the mixed $CH_4 + C_3H_8$ clathrate hydrate equilibria in silica gel pores: Effects of pore size and salinity. *Langmuir* **2010**, *26*, 9742–9748. [CrossRef]

23. Liu, H.; Zhan, S.; Guo, P.; Fan, S.; Zhang, S. Understanding the characteristic of methane hydrate equilibrium in materials and its potential application. *Chem. Eng. J.* **2018**, *349*, 775–781. [CrossRef]

24. Zhou, J.; Liang, W.; Wei, C. Phase equilibrium condition for pore hydrate: Theoretical formulation and experimental validation. *J. Geophys. Res. Solid Earth* **2019**, 124. [CrossRef]

25. Liang, W.; Zhou, J.; Wei, C. Uniqueness of the equilibrium relationship among temperature, pressure and liquid water content in hydrate-bearing soils. *J. Nat. Gas Sci. Eng.* **2021**, *88*, 103820. [CrossRef]

26. Azimi, A.; Javanmardi, J.; Mohammadi, A.H. Development of thermodynamic frameworks for modeling of clathrate hydrates stability conditions in porous media. *J. Mol. Liq.* **2021**, *329*, 115463. [CrossRef]

27. Zhang, Y.; Taboada-Serrano, P. Model for gas-hydrate equilibrium in porous media that incorporates pore-wall properties. *Phys. Chem. Chem. Phys.* **2020**, *22*, 10900–10910. [CrossRef] [PubMed]

28. Istomin, V.A.; Chuvilin, E.M.; Bukhanov, B.A.; Uchida, T.A. Pore water content in equilibrium with ice or gas hydrate in sediments. *Cold Reg. Sci. Technol.* **2017**, *137*, 60–67. [CrossRef]

29. Chuvilin, E.V.; Istomin, V.A.; Safonov, S.S. Residual nonclathrated water in sediments in equilibrium with gas hydrate, Comparison with unfrozen water. *Colds Reg. Sci. Technol.* **2011**, *68*, 68–73. [CrossRef]

30. Chuvilin, E.; Istomin, V. Temperature dependence of the equilibrium pore water content in gas hydrate contained sediments. *Proc. Tenth Int. Conf. Permafr.* **2012**, *2*, 57–60.

31. Yakushev, V.S. Experimental modeling of methane hydrate formation and decomposition in wet heavy clays in Arctic regions. *Geosciences* **2019**, *9*, 13. [CrossRef]

32. Sell, K.; Quintal, B.; Kersten, M.; Saenger, E.H. Squirt flow due to interfacial water films in hydrate bearing sediments. *Solid Earth* **2018**, *9*, 699–711. [CrossRef]

33. Hansen, T.C.; Falenty, A.; Kuhs, W.F. Lattice constants and expansivities of gas hydrates from 10 K up to the stability limit. *J. Chem. Phys.* **2016**, *144*, 054301. [CrossRef]

34. Istomin, V.A.; Chuvilin, E.M.; Bukhanov, B.A. Fast estimation of unfrozen water content in frozen soils. *Earth's Cryosphere* **2017**, *21*, 116–120. [CrossRef]

35. Sloan, D.E. *Clathrate Hydrates of Natural Gases*; Marcel Dekker: New York, NY, USA, 1990; p. 641.

36. Istomin, V.A.; Yakushev, V.S. *Natural Gas Hydrates*; Nedra: Moscow, Russia, 1992; p. 236. (In Russian)

37. Broseta, D.; Ruffine, L.; Desmedt, A. *Gas Hydrates 1: Fundamentals, Characterization and Modeling*; Wiley-ISTE: London, UK, 2017; p. 302.

38. Luo, T.; Li, Y.; Sun, X.; Shen, S.; Wu, P. Effect of sediment particle size on the mechanical properties of CH_4 hydrate-bearing sediments. *J. Pet. Sci. Eng.* **2018**, *171*, 302–314. [CrossRef]

39. Krichevsky, I.R.; Kazarnovsky, Y.S. On thermodynamics of equilibrium gas-gas solution in liquid. *J. Phys. Chem.* **1935**, *6*, 1320–1324.

40. Namiot, A.Y. *Gas Solubility in Water*; Nedra: Moscow, Russia, 1991; p. 167. (In Russian)

41. Mel'nikov, V.P.; Nesterov, A.N.; Reshetnikov, A.V.; Istomin, V.A.; Kwon, V.G. Stability and growth of gas hydrates below the ice-hydrate-gas-equilibrium line on the P-T-phase diagram. *Chem. Eng. Sci.* **2010**, *65*, 906–914. [CrossRef]

42. Mel'nikov, V.P.; Nesterov, A.N.; Reshetnikov, A.V.; Istomin, V.A. Metastable state during dissociation of carbon dioxide hydrates below 273 K. *Chem. Eng. Sci.* **2011**, *66*, 73–77. [CrossRef]

43. Istomin, V.; Kwon, V.; Kolushev, N.; Kulkov, A. Prevention of gas hydrate formation at field conditions in Russia. In Proceedings of the 2-nd International Conference on Natural Gas Hydrates, Toulouse, France, 2–6 June 1996; pp. 399–406.

44. Istomin, V.A.; Chuvilin, E.M.; Makhonina, N.A.; Bukhanov, B.A. Temperature dependence of unfrozen water content in sediments on the water potential measurements. *Cryosphere Earth* **2009**, *13*, 35–43. (In Russian)

45. Chuvilin, E.M.; Gureeva, O.M.; Istomin, V.A.; Safonov, S.S. Experimental method for determination of the residual equilibrium water content in hydrate-saturated natural sediments. In Proceedings of the 6th International Conference on Gas Hydrates (ICGH 2008), Vancouver, BC, Canada, 6–10 July 2008; p. 5490.
46. Chuvilin, E.M.; Istomin, V.A.; Safonov, S.S. Method for Determination of Pore Water Content in Equilibrium with Gas Hydrate in Dispersed Media. U.S. Patent 2010/0139378 A1, 10 June 2010.